PHYSICAL REVIEW B **68**, 155317 (2003)

Effect of an additional infrared excitation on the luminescence efficiency of a single InAs/GaAs quantum dot

E. S. Moskalenko,[1,2] V. Donchev,[1,3] K. F. Karlsson,[1] P. O. Holtz,[1] B. Monemar,[1] W. V. Schoenfeld,[4] J. M. Garcia,[4] and P. M. Petroff[4]

[1]*Department of Physics and Measurement Technology, Linköping University, S-581 83 Linköping, Sweden*
[2]*A.F. Ioffe Physical-Technical Institute, RAS, 194021, Polytechnicheskaya 26, St. Petersburg, Russia*
[3]*Faculty of Physics, Sofia University, 5, blvd. James Bourchier, 1164-Sofia, Bulgaria*
[4]*Materials Department, University of California, Santa Barbara, California 93106, USA*

(Received 29 April 2003; revised manuscript received 11 July 2003; published 20 October 2003)

Microphotoluminescence (PL) spectra of a single InAs/GaAs self-assembled quantum dot (QD) are studied under the main excitation of electron-hole pairs in the wetting layer (WL) and an additional infrared (IR) laser illumination. It is demonstrated that the IR laser with fixed photon energy well below the QD ground state induces striking changes in the spectra for a range of excitation energies and powers of the two lasers. For the main excitation above a threshold energy, defined as the onset of transitions between shallow acceptors and the conduction band in GaAs, the addition of the IR laser will induce a considerable increase in the QD emission intensity. This is explained in terms of additional generation of extra electrons and holes into the QD by the two lasers. For excitation below the threshold energy, the carrier capture efficiency from the WL into the QD is suggested to be essentially determined by the internal electric-field-driven carrier transport in the plane of the WL. The extra holes, generated in the GaAs by the IR laser, are supposed to effectively screen the built-in field, which results in a considerable reduction of the carrier collection efficiency into the QD and, consequently, a decrease of the QD PL intensity. A model is presented which allows estimating the magnitude of the built-in field as well as the dependence of the observed increase of the QD PL intensity on the powers of the two lasers. The use of an additional IR laser is considered to be helpful to effectively manipulate the emission efficiency of the quantum dot, which could be used in practice in quantum-dot-based optical switches.

DOI: 10.1103/PhysRevB.68.155317 PACS number(s): 78.67.Hc, 71.55.Eq, 78.66.Fd

I. INTRODUCTION

Semiconductor quantum dots (QD's), which may be referred to as ''artificial atoms,'' [1] are of great contemporary interest mainly for their current and future applications in practice as a variety of optoelectronic (electronic) devices, such as QD lasers,[2] QD infrared detectors,[3] QD memory devices,[4] and single-electron transistors.[5] In most of the experiments the QD's are populated with carriers, which are primarily created somewhere in the sample [in the barriers or in the wetting layer (WL), on which QD's are normally grown [6]]—i.e., outside the QD's—by means of electrical or optical excitation. This highlights the crucial role of the carrier capture processes into the QD for the performance and operation of QD-based devices. Indeed, a more effective capture will result in a higher population of carriers and excitons in the QD, which increases its radiative efficiency. However, the capture could also be considerably affected by the impurities, positioned in the barriers and/or WL, giving rise to a nonradiative recombination. Consequently, detailed studies of both the properties of the surrounding media and the carrier capture mechanisms are needed to achieve in practice a high emission from the QD.

The carrier capture mechanisms intensively studied in the last decade reveal optical phonon assisted,[7,8] Auger-like,[9] and shake-up[10] processes and carrier relaxation through the band tail states of the WL with a subsequent emission of localized phonons.[11] The lateral carrier transport (in the plane of the WL) could be affected by carrier hopping between QD's,[12] by trapping of migrating particles into localized states of the WL (Ref. 13) or into nonradiative centers (Ref. 14) in the surrounding media. In analogy, a magnetic field directed perpendicular to the plane of the structure will limit the lateral transport.[15]

It has also been suggested[7] that the carrier drift could be considerably influenced by a long-range attractive potential caused by the strain field surrounding the QD. On the other hand, strain-induced potential barriers in the barrier/QD (Ref. 16) and WL/QD (Ref. 17) interfaces were considered to limit the carrier capture into the QD. The important role of the electric field directed in the growth direction of the sample on carrier capture into and escape out of the QD was demonstrated by the studies of the electric current passing through the QD's.[18]

A number of effects of the surrounding defects on the carriers and excitons in the QD have been reported up to now: e.g., defect-assisted relaxation of carriers inside a QD,[19] supplying the QD with electrons from the donor atoms,[20] blinking,[21] and spectral diffusion[22] phenomena. An enhancement by one order of magnitude of the recombination efficiency of InAs/GaAs QD's when a tunneling barrier was introduced between the InAs layer and GaAs cap layer has been reported[23] and explained in terms of an effective suppression of the nonradiative transitions in the WL.

In our previous study,[24] a faster capture of electrons (e's) into a single InAs QD compared to the holes (h's) was demonstrated. The capture rate was strongly dependent on the excitation energy $h\nu_{ex}$ used. This fact allowed us to identify a number of novel lines in the photoluminescence (PL) spec-

tra of a single QD as being due to negatively charged exciton complexes.

In the present paper, we demonstrate the important role of another mechanism, the built-in electric field F directed in the plane of a WL, which has not been previously considered. This field determines the carrier capture rate into the QD for the experimental conditions when carriers are excited in the WL (below the barriers) and, consequently, they can approach the location of the QD only by moving along the plane of the WL. Carriers, excited into the WL, are subjected to this field and can, accordingly, acquire a field-dependent transport. Consequently, the individual carriers are able to reach the QD before forming an exciton in the WL, which results in a rather high PL signal of the QD, $I_{\mathrm{PL}}^{\mathrm{QD}}$, relative to the intensity of the WL emission. The presence of the field F is considered to be due to defect atoms (donors and acceptors) located at the WL/barrier interface. The existence of such defects at the InAs/GaAs interface was experimentally demonstrated.[14]

In our experiments we use an additional infrared (IR) laser to influence the field F. The excitation energy of the IR laser, $h\nu_{\mathrm{IR}}=1.233$ eV, is considerably less than the lowest transition energy of the sample studied and, accordingly, cannot excite free carriers [electrons (e's) and holes (h's)] as a result of the band-to-band absorption. e's or h's can solely be created due to excitation of deep level (DL) defects positioned in the band gap of the GaAs barriers.[25] According to our model, these extra carriers, excited in the sample by the IR laser, effectively screen the field F and, consequently, the carrier transport in the plane of the WL is slowed down. Due to the screened field, a considerable (up to 20 times) reduction of $I_{\mathrm{PL}}^{\mathrm{QD}}$ is experimentally observed when the sample is doubly excited both with an IR laser and a main laser with $h\nu_{ex}$ above the band gap energy of the WL.

To the best of our knowledge, there is only one publication[26] devoted to studies of IR laser induced changes in the PL of QD's. It was found that the IR laser induces an increase of the PL from the QD's by up to 40%. This phenomenon was explained in terms of an IR-laser-induced release of carriers, which were trapped into deep defects from the QD's. These experiments[26] were carried out for a large ensemble of InAs/GaAs QD's of a rather high density, which prevents the simultaneous measurements of the PL from the WL and the details of the PL spectra from an individual QD. Consequently, the observed increase of the QD's PL intensity[26] may not necessarily be due to the mechanism of carrier capture into a defect from a QD. The same phenomenon could be registered assuming that carriers $e(h)$ have been trapped into the defects from the conduction (valence) band of the WL on their way to the QD. Then the IR laser could release these trapped carriers increasing the PL of both the QD and WL. Such an enhancement of the radiative efficiency, induced by an additional below band gap excitation, is well known.[27]

In the present paper, we have studied the PL spectra of a single InAs/GaAs QD; i.e., only one QD is located within the laser spot. Accordingly, the PL emission of both the WL and QD can be monitored simultaneously. This allows us to distinguish between different mechanisms due to the influence of the IR laser on the PL of the sample: the suppression of the nonradiative recombination in the WL and the influence on the collection efficiency of the QD.

The above described effect of the reduction of $I_{\mathrm{PL}}^{\mathrm{QD}}$, induced by an additional IR laser, was registered for excitation energies $h\nu_{ex}$'s of the main laser in the range of $h\nu_{me}<h\nu_{ex}<h\nu_{th}$ ($h\nu_{th}<E_{\mathrm{X}}^{\mathrm{GaAs}}$) where $E_{\mathrm{X}}^{\mathrm{GaAs}}$ is the energy of the free exciton transition in the GaAs barriers. $h\nu_{me}$ is the mobility edge determined by the onset of the heavy-hole peak measured in the PL excitation spectrum of the WL and $h\nu_{th}$ is the threshold energy. The threshold energy has been identified[28] as the energy, above which additional negative charge carriers can be accumulated in the QD, which gives rise to the observation of the negatively charged exciton in the PL spectra of individual QD's. This phenomenon was ascribed[28] to the acceptor to the conduction band transitions in GaAs, which causes an effective generation of surplus free e's in the sample.

Surprisingly, for main laser excitation energies of $h\nu_{th}<h\nu_{ex}<E_{\mathrm{X}}^{\mathrm{GaAs}}$, the additional IR laser induces an essential increase (5–6 times) of $I_{\mathrm{PL}}^{\mathrm{QD}}$. In addition, the PL spectra are redistributed in favor of the neutral exciton. This fact is evidence for the creation of surplus holes in the sample, which, in turn, allows us to explain the increase of $I_{\mathrm{PL}}^{\mathrm{QD}}$ in terms of an additional separate generation of surplus e's and h's upon simultaneous excitation of two lasers.

We also present experimental results for double-laser-excited PL, when the two laser spots were spatially separated: The IR laser was positioned on the QD while the spot of the main laser was moved aside (2.5 μm) from the QD. For this excitation geometry, each laser gave an undetectable contribution to the PL spectrum, when exciting separately, but a very efficient PL signal was registered upon simultaneous excitation. This observation serves, in our opinion, as a direct experimental proof for the generation of extra e's and h's by the two lasers. The effect of the IR-laser-stimulated generation of holes into the QD has earlier been demonstrated[29] for the case of InP/GaInP samples. The PL signal from the QD was registered when the sample was illuminated with the light of an IR laser, in addition to the electric current passing through the QD's.

We were not able to detect any change (increase or decrease) in the QD PL signal, induced by the IR laser, for excitation with $h\nu_{ex}<h\nu_{me}$—i.e., when the QD was excited directly. This allows us to exclude a possible influence of the nonradiative centers, which were considered to play an important role for carriers already captured into the QD.[26,29]

The suggested model explains the majority of the experimental data obtained. In particular, we can estimate the internal electric field needed to account for the observed quenching of $I_{\mathrm{PL}}^{\mathrm{QD}}$, as well as to predict the observed dependence of the increase of the PL signal from the QD on the powers of the two lasers. The use of an additional IR laser is considered to be an original tool to effectively manipulate (increase or decrease) the luminescence efficiency from the QD's, which could be employed in applications: e.g., QD-based optical switches.

II. SAMPLES AND EXPERIMENTAL SETUP

The samples studied were grown by molecular beam epitaxy (MBE) on a semi-insulating GaAs (100) substrate. The buffer layer was prepared with a short-period superlattice 40×2 nm/2 nm AlAs/GaAs at a growth temperature of 630 °C. On top of a 100-nm GaAs layer the QD's were formed from about 1.7 InAs monolayers layer deposited at 530 °C. A first growth interruption of 30 s was used to improve the size distribution. Then the dots were covered with a thin GaAs cap layer with a thickness of $t_{\mathrm{cap}}=3$ nm before a crucial second growth interruption of 30 s. Finally, a 100-nm-thick GaAs layer was deposited to protect the QD's. Transmission electron microscopy studies of analogously grown samples revealed that uncapped original dots are lens (hemispherical) shaped with a typical lateral size of 35 nm and a height of 10 nm.[6] The deposition of a GaAs capping layer after the dots have been formed with $t_{\mathrm{cap}}=3$ nm leads to an essential reduction in the QD's height down to 4.5 nm. Consequently, the PL is blueshifted to the spectral region of 1.34 eV ($\sim$950 nm) (Ref. 6)—i.e., within the sensitivity spectral range of the Si charge-coupled-device (CCD) camera. The sample was grown without rotation of the substrate, so that a gradual variation of In flux is achieved across the wafer, resulting in a gradient in both the density and average size of the dots across the epitaxial layer.[6]

The QD's were studied by means of a conventional diffraction-limited micro-PL (μPL) setup. To excite the QD's, we used two cw Ar-laser-pumped Ti-Sp lasers. One of them, which was used to excite the PL in the QD, was tuned from 730 to 880 nm, while the other laser was set to a fixed wavelength of 1005 nm. The excitation power of the two lasers was adjusted by the use of neutral density filters. The beams of the two Ti-Sp lasers were focused on the sample surface by a microscope objective through a thin optical window of a continuous-flow cryostat. The experiments were carried out at a temperature of 5 K. The laser beams could be focused on the sample surface down to a spot size of 2 μm in diameter. The luminescence signal was collected by the same objective and dispersed by a single-grating 0.45-m monochromator combined with a LN_2-cooled Si-CCD camera. The spectral resolution achieved in the region of the studied PL was 0.15 meV. For the PL excitation (PLE) measurements, a double-grating 0.85-m monochromator was used in combination with a LN_2-cooled InGaAsP photomultiplier.

To find the particular QD to study, a laser beam was scanned across the sample surface. Once the desired QD was found, special marks (grids) were fabricated on the sample surface around the QD with a laser beam of a very high power density. This allowed us to estimate the average distance between adjacent QD's to be around 10 μm in the studied QD structure. To control the exact position of the laser spot on the sample surface, the image of the interesting sample region was projected on a video camera, which made it easy to find the desired QD by using the fabricated marks. In addition, this arrangement allowed us to effectively correct the laser position on the sample, if the sample was moved due to the thermal drift. It should be noted that with this method to locate the exact QD position by using the described grids, one can avoid some undesirable consequences, which take place with other methods. For example, when a metal mask with small holes is deposited on top of the sample, it may produce an electric field in the near-surface region of the sample and, consequently, may influence the carrier transport in the plane of the WL. In addition, the metal mask may act as a stressor, which could spoil the entire quality of the QD's.

Eight single QD's located at different spatial positions of the sample were examined in this study. All of them revealed an analogous behavior with respect to the IR-laser-induced changes in the PL spectra and, for consistency, we present data measured on one specific QD.

III. EXPERIMENTAL RESULTS AND DISCUSSION

Figure 1(a) shows a low-temperature μPL spectrum of a sample (solid line) and a macro-PLE spectrum of the WL (dotted line), taken at the conditions given in the figure caption. The PL spectrum is dominated by the PL WL emission, which is centered around an energy of 1.445 eV. The PLE spectrum is dominated by the peak marked as $E_{\mathrm{X}}^{\mathrm{GaAs}}$, which is due to the free exciton absorption in the GaAs barriers. Two broad PLE bands marked as $E_{\mathrm{HH}}^{\mathrm{WL}}$ and $E_{\mathrm{LH}}^{\mathrm{WL}}$ are also distinctly resolved and attributed to the absorption of the electron-to-heavy/light-hole transitions, respectively, in the WL. This assignment was done in our previous work[28] on the basis of μPLE measurements on the cleaved edge of the sample, performed with different (parallel and perpendicular) directions of the laser polarization with respect to the sample plane.

The μPL spectrum shown in Fig. 1(a) also reveals a contribution originating from the emission of a single QD under study. It consists of two groups of PL lines centered around 1.34 eV and 1.37 eV and marked as s-s and p-p, respectively. The s-s (p-p) PL lines originate from the radiative recombination of electrons e's and holes h's captured to the ground (first excited) energy level of a single QD, as was shown in our previous work.[24] In the following we will concentrate on the studies of the details of the s-s PL lines and on the changes introduced by an additional illumination of an IR laser, L_{IR}. In the present paper, we will also restrict ourselves to the studies of the PL of the QD in the excitation energy $h\nu_{ex}$ region below the $E_{\mathrm{X}}^{\mathrm{GaAs}}$. The results obtained for the case of $h\nu_{ex}>E_{\mathrm{X}}^{\mathrm{GaAs}}$ (not shown here) will be shortly summarized and commented in the end of this section.

Figures 1(b)–1(e) show four pairs of PL spectra of a single QD recorded at $T=5$ K and a number of $h\nu_{ex}$'s of the main laser L_0, shown for the convenience by the solid curved arrows in Fig. 1. Each pair of PL spectra consists of a spectrum excited with only L_0 at an excitation power of $P_0=100$ nW (solid line) together with a spectrum recorded with an additional excitation of an IR laser at an excitation power of $P_{\mathrm{IR}}=50$ μW [dotted lines in Figs. 1(b)–1(e)]. We discuss first the PL spectra measured with excitation from a single laser L_0. It is seen [solid lines in Figs. 1(b)–1(e)] that the PL spectra consist mainly of the three PL lines marked as X, $X-$, and $X--$, which relative intensities in each par-

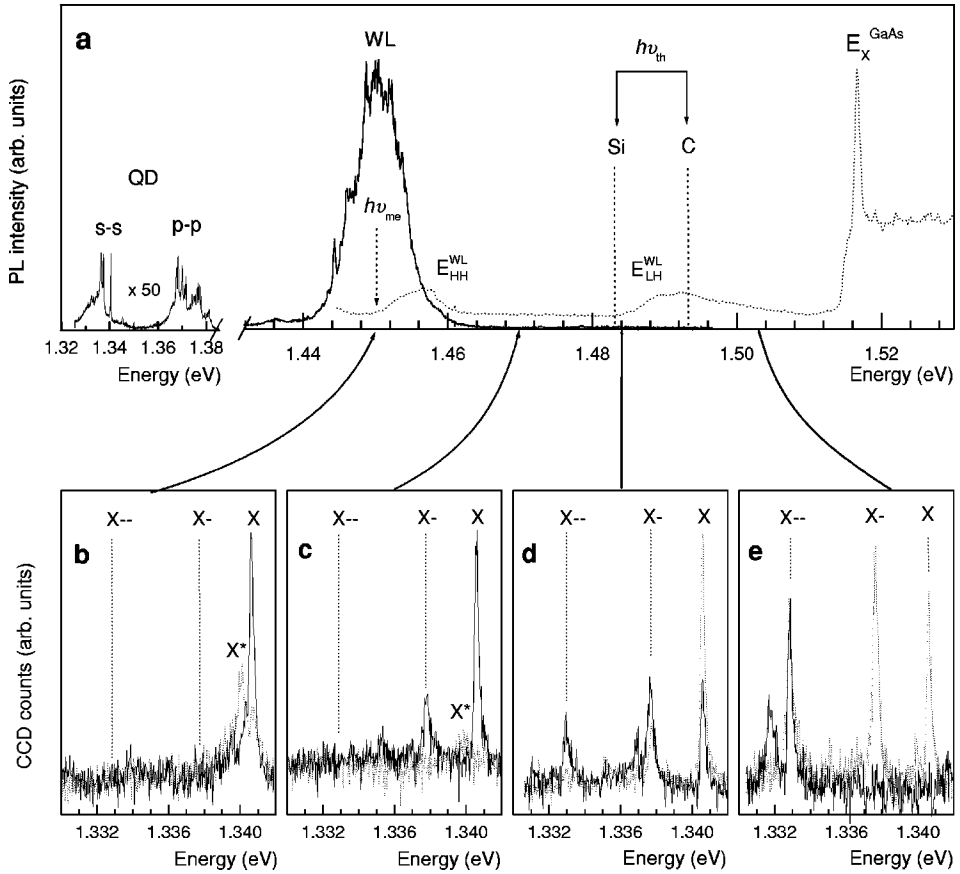

FIG. 1. (a) μPL spectra of a single QD and the WL (solid lines) measured at $T=5$ K, $h\nu_{ex}=1.684$ eV, and an excitation power of $P_0=410$ nW. The dotted line shows the macro-PLE spectrum of the WL measured from a large $(50\ \mu\text{m})^2$ sample area around the QD at $T=5$ K and $P_{ex}=50$ mW. The PLE spectrum is obtained by detection at 1.441 eV. The vertical dotted arrow and the two vertical dotted lines show the energy positions of the mobility edge and the threshold energies for the Si and C acceptors, respectively. Four pairs of PL spectra, measured on the single QD at $T=5$ K with a single (double) laser, are shown by the solid (dotted) lines for an excitation energy (b) $h\nu_{ex}=1.450$ eV, (c) 1.470 eV, (d) 1.484 eV, and (e) 1.503 eV, respectively, and an excitation power of $P_0=100$ nW and $P_{IR}=50\ \mu$W. Each pair of PL spectra (b)–(e) was normalized to the maximum value of the PL amplitude of the strongest spectrum. The curved solid arrows indicate, for convenience, the exact value of $h\nu_{ex}$ at which each of the pairs (b)–(e) was measured.

ticular PL spectrum are dramatically dependent on the exact value of the $h\nu_{ex}$ used.

The origin of these PL lines has been revealed in our previous work,[24] where we studied the PL spectra of the same single QD at a number of $h\nu_{ex}>E_X^{GaAs}$. The studies allow us to interpret these as being due to the neutral (X), single $(X-)$, and double negatively $(X--)$ charged excitons, which correspond to the situation when the QD is occupied with $1e1h$, $2e1h$, and $3e1h$ charge configurations, respectively. The reason for the appearance of an extra charge in the QD was considered as a more efficient capture of the photoexcited e's into the QD with respect to the capture of h's. Each PL spectrum in Figs. 1(b)–1(e) was recorded with an integration time of tens of seconds, which is much longer than the typical value of the exciton recombination time ($\sim 10^{-9}$ s) in InAs QD's (Ref. 12) and in InAs quantum wells (Ref. 30). Correspondingly, the detected PL intensity distribution of these three lines simply reflects the probability, averaged on a long time scale, for the QD to have a definite charge configuration at a given time instant. The appearance of the $X--$ and $X-$ lines, redshifted with respect to the line X, is consistent with the theoretical predictions[31] and the experimental observations by other authors.[20,32,33]

In a more recent study[28] we thoroughly investigated the PL spectra of the QD at a number of $h\nu_{ex}<E_X^{GaAs}$. A novel phenomenon was revealed. For $h\nu_{ex}$ greater than the threshold energy $h\nu_{th}$, the PL spectra of the QD entirely consisted of a single $X--$ line, while at $h\nu_{ex}<h\nu_{th}$ X line dominated the PL spectra. This phenomenon was ascribed to the effect of the generation of the surplus e's from the acceptor atoms (processes shown by arrow 3 in Fig. 2), positioned in the GaAs barriers. Correspondingly, $h\nu_{th}=E_g^{GaAs}-E_a$, where $E_g^{GaAs}=1.519$ eV is the band gap energy of the GaAs at $T=5$ K and E_a is the binding energy of the acceptor atom (Fig. 2). It should be mentioned that the two threshold energies $h\nu_{th}^{Si}$ and $h\nu_{th}^{C}$ shown by a vertical dotted lines in Fig. 1(a) were revealed in Ref. 28. These are due to the presence of different type of acceptors Si and C in the GaAs barriers, respectively.

At excitations with $h\nu_{ex}>h\nu_{th}$, an equal number of e's

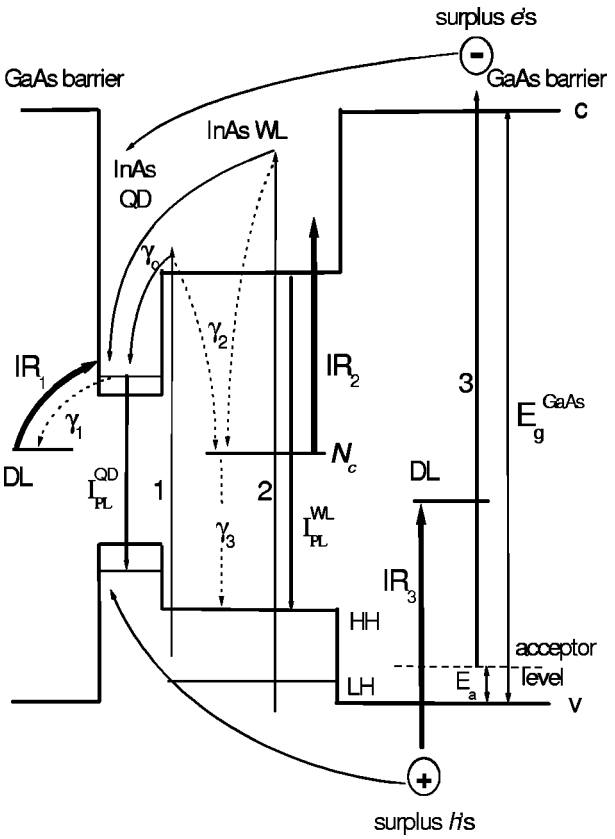

FIG. 2. The conduction band (c) and valence band (v) edges in the growth direction of the sample structure together with the acceptor and defect level (DL) positions in the sample studied. Arrows 1, 2, and 3 indicate the heavy-hole, light-hole, and acceptor-to-conduction band transitions, respectively. The thick solid arrows IR_1, IR_2, and IR_3 correspond to the photoionization processes of the captured excitons from the DL into the QD, from the defect into the WL, and the generation of surplus holes in the GaAs valence band, respectively. The curved arrows γ_1, γ_2, γ_c, and γ_3 indicate the capture processes of the excitons into the DL from the QD, from the WL into the defect, the exciton capture from the WL into the QD, and the recombination of excitons trapped by the defect, respectively. Also the energies of the GaAs band gap (E_g^{GaAs}) and the acceptor binding energy (E_a) are shown.

and *h*'s are created as a result of the absorption of the photons in the WL (processes shown by arrow 2 in Fig. 2) and, in addition, a surplus of *e*'s can be excited as a result of the absorption of other photons of the same laser in the GaAs barriers (processes shown by arrow 3 in Fig. 2). This explains the appearance of the "negative" charge configuration in the QD at $h\nu_{ex} > h\nu_{th}$. Correspondingly, a "neutral" charge state is expected in the QD at excitations at $h\nu_{ex} < h\nu_{th}$, which provides an equal amount of photoexcited *e*'s and *h*'s in the WL (processes shown by arrow 1 in Fig. 2).

An additional IR laser L_{IR} initiates a dramatic change in the PL spectra, which is shown for some illustrative excitation conditions by dotted lines in Figs. 1(b)–1(e). These changes are entirely determined by the exact value of the $h\nu_{ex}$ of the main laser L_0. The solid line in Fig. 1(e) shows the PL spectrum taken with a single L_0 at $h\nu_{ex} > h\nu_{th}$. It consists of the $X--$ line and an additional line redshifted by 1.5 meV. The latter line is considered to correspond to the $4e1h$ configuration of the QD.[31] It is more clearly revealed in the PL spectrum in Fig. 1(e) with respect to the PL spectra measured in Ref. 28 due to a larger $P_0 = 100$ nW used in the present study compared to the value of the P_0 employed previously. It is clear that the additional IR laser redistributes the PL spectrum in favor of the $X-$ and X PL lines [dotted line in Fig. 1(e)]. Another remarkable feature is that the total PL intensity of the QD, I_{PL}^{QD}, integrated over the entire spectral region, becomes 2 times higher with respect to the case when the PL spectrum was excited with a single laser L_0 [Fig. 1(e)]. Qualitatively the same behavior is observed for excitations with $h\nu_{ex} = 1.484$ eV [Fig. 1(d)] with the only difference that I_{PL}^{QD} remains the same.

For excitations with $h\nu_{ex} < h\nu_{th}$ the IR laser influences the PL spectra in a completely opposite way compared to the case of excitation with $h\nu_{ex} > h\nu_{th}$. PL spectra, taken with only L_0, consist mainly of the line X [solid lines in Figs. 1(b) and 1(c)], as expected for the excitation conditions which provide equal amount of *e*'s and *h*'s excited in the WL (arrow 1 in Fig. 2). The small contribution to the $X-$ line, seen in Fig. 1(c), can be explained in terms of the faster capture of *e*'s into the QD, analogously to the considerations described in detail in Ref. 24. The PL spectrum, taken at $h\nu_{ex} = 1.470$ eV [Fig. 1(c)], undergoes a considerable quenching when the IR laser is switched on [compare solid and a dotted lines in Fig. 1(c)].

Another effect was registered, when the $h\nu_{ex}$ was set at the energy of the mobility edge $h\nu_{me}$, defined as the onset of the E_{HH}^{WL} PLE band and shown by a vertical dotted arrow in Fig. 1(a). The PL spectrum taken with only L_0 consists solely of the neutral exciton line X [solid line in Fig. 1(b)]. The addition of the L_{IR} leaves I_{PL}^{QD} unchanged, but initiates the appearance of a new line X^* redshifted by 0.8 meV with respect to the line X, which is demonstrated by the PL spectrum shown by a dotted line in Fig. 1(b). The possible origin of the line X^* will be discussed in the end of this section. Here we note that a small contribution of the same line X^* to the PL spectrum excited with both lasers could also be distinguished in Fig. 1(c).

It is very important to note that the addition of the IR laser does not change the total PL intensity I_{PL}^{QD} at any value of the $h\nu_{ex}$ in the studied range of $1.408\ \text{eV} < h\nu_{ex} < h\nu_{me}$ (these results are not shown here), while it initiates a considerable decrease (increase) of I_{PL}^{QD} at any value of $h\nu_{ex}$ in the range $h\nu_{me} < h\nu_{ex} < h\nu_{th}^{Si}$ ($h\nu_{ex} > h\nu_{th}^{C}$). It should be mentioned that the excitation energy of the IR laser, $h\nu_{IR} = 1.233$ eV, is well below the energy of the ground-state transition of the QD (≈ 1.34 eV). Consequently, no contribution to the PL spectra either of the QD or of the WL is expected exciting with only L_{IR}, which is in full agreement with what was observed in the experiment (not shown here).

The detected changes in the PL spectra [Figs. 1(d) and 1(e)], initiated by the IR laser, can only be understood in terms of the extra hole appearance in the sample as a result of the IR excitation. A possible reason for these processes could be transitions of electrons from the valence band of the GaAs barriers to the DL's located in the band gap of GaAs

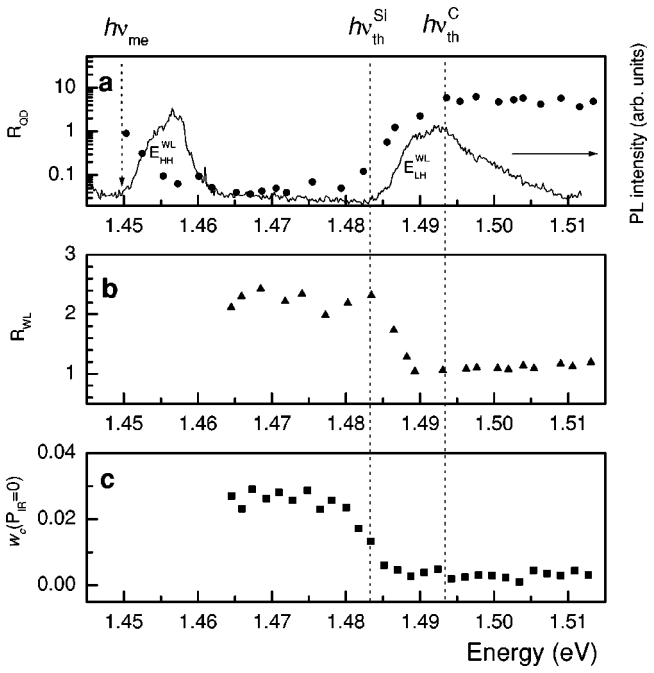

FIG. 3. The ratio of the spectrally integrated PL intensity measured at $T=5$ K with both lasers and the integrated PL intensity measured with only one laser (L_0), R_{QD} and R_{WL}, respectively, for (a) the QD and (b) the WL. The excitation powers of $P_0=20$ nW and $P_{\mathrm{IR}}=50\ \mu$W were used to excite these PL spectra. The PLE spectrum of the WL [same as in Fig. 1(a)] is also shown. (c) The ratio between the spectrally integrated PL intensities of the QD and the WL $w_c(P_{\mathrm{IR}}=0)$ measured at $T=5$ K, $P_0=20$ nW, and $P_{\mathrm{IR}}=0$. The vertical dotted arrow and the two lines have the same meaning as in Fig. 1(a).

(these are shown by the arrow marked IR_3 in Fig. 2). The existence of such DL's in both bulk[25] and MBE-grown[14] GaAs is well known. Thus, it is reasonable to expect that the appearance of the surplus h's, initiated by the absorption of the IR laser, will effectively ''neutralize'' the QD. But there are two alternatives, which could be responsible for such a behavior. On the one hand, the surplus h's could compensate the extra e's inside the QD—i.e., to neutralize those e's which have already been captured into the QD in the experiments with a single laser L_0. On the other hand, this compensation could take place in the volume of the WL or inside the GaAs barriers. Our experimental results, as will be shown below, allow us to conclude that the neutralization takes place in the QD.

To summarize the experimental data described, L_{IR} initiates a redistribution of the PL spectra, but causes also considerable changes of $I_{\mathrm{PL}}^{\mathrm{QD}}$. Accordingly, the following data will be presented in terms of the rate R_{QD}, defined as the ratio between $I_{\mathrm{PL}}^{\mathrm{QD}}$ measured with both lasers and the spectrally integrated intensity measured with only a single laser L_0 employed. Figure 3(a) shows the values of R_{QD} measured at $T=5$ K, $P_0=20$ nW, $P_{\mathrm{IR}}=50\ \mu$W, and a number of $h\nu_{ex}$'s. A PLE spectrum from Fig. 1(a) is also shown here for comparison and further analysis. It is seen [Fig. 3(a)] that R_{QD} reveals different values depending on the exact value of $h\nu_{ex}$. In the region of $h\nu_{ex}>h\nu_{th}^{\mathrm{C}}$, $R_{\mathrm{QD}}>1$, while R_{QD} acquires values well below 1 at $h\nu_{ex}<h\nu_{th}^{\mathrm{Si}}$, monotonously changing in the intermediate region of $h\nu_{th}^{\mathrm{Si}}<h\nu_{ex}<h\nu_{th}^{\mathrm{C}}$ [Fig. 3(a)]. It is also seen that R_{QD} gradually increases up to 1 when $h\nu_{ex}$ is progressively reduced in the spectral region of the heavy-hole PLE band of the WL [Fig. 3(a)]. The value of R_{QD} has been found to be equal to 1 at a number of $h\nu_{ex}<h\nu_{me}$, as was explained above. These results are not shown in Fig. 3(a), because the corresponding PL spectra were measured with values of P_0, which were considerably higher (≈ 100 times) than the $P_0=20$ nW, to compensate for the sharp decrease of the density of the absorbing states.

Figure 3(b) shows the rate R_{WL}, which is defined analogously to the above-introduced R_{QD}, calculated for the intensity of the spectrally integrated WL emission, $I_{\mathrm{PL}}^{\mathrm{WL}}$, as a function $h\nu_{ex}$. It also reveals different values, which are as much as 2.5 at $h\nu_{ex}<h\nu_{th}^{\mathrm{Si}}$, progressively reducing in magnitude down to approximately 1.1 at $h\nu_{ex}>h\nu_{th}^{\mathrm{C}}$. Figure 3(c) shows the quantity of $w_c(P_{\mathrm{IR}}=0)$, defined as the ratio $I_{\mathrm{PL}}^{\mathrm{QD}}/I_{\mathrm{PL}}^{\mathrm{WL}}$, calculated for the case of excitation with only L_0 at $T=5$ K and $P_0=20$ nW. It is seen [Fig. 3(c)] that $w_c(P_{\mathrm{IR}}=0)$ has a very low value (≈ 0.003) at $h\nu_{ex}>h\nu_{th}^{\mathrm{C}}$, progressively increasing up to ≈ 0.03 with a decrease of $h\nu_{ex}$. It should be mentioned that we were forced to use $h\nu_{ex}=1.464$ eV as the lowest excitation energy for the cases of Figs. 3(b) and 3(c), because our present experimental setup, with a single-grating monochromator, gives a considerable background contribution to the WL PL band from the laser at $h\nu_{ex}<1.464$ eV. Consequently, we were not able to determine the exact values of $I_{\mathrm{PL}}^{\mathrm{WL}}$ in this excitation region.

As follows from the described experimental data, summarized in Fig. 3(a), there are three main regions of the $h\nu_{ex}$'s within which L_{IR} influences the PL spectra in a completely different way: the first is at $h\nu_{ex}\leqslant h\nu_{me}$ where $R_{\mathrm{QD}}=1$, the second is at $h\nu_{me}<h\nu_{ex}<h\nu_{th}^{\mathrm{Si}}$, which reveals $R_{\mathrm{QD}}<1$, and the last one is at $h\nu_{th}^{\mathrm{C}}<h\nu_{ex}<E_{\mathrm{X}}^{\mathrm{GaAs}}$, where $R_{\mathrm{QD}}>1$. Consequently, it is natural to expect that different mechanisms are responsible for the observed phenomena for these different regions of $h\nu_{ex}$.

A. $h\nu_{ex}\leqslant h\nu_{me}$

We start first with the region of $h\nu_{ex}\leqslant h\nu_{me}$. As follows from the studies of other authors,[26,29] it is expected that the carriers and excitons, captured into the QD, can tunnel from the dot to a defect atom or DL located in the close vicinity of the QD prior to the radiative recombination, giving rise to a nonradiative recombination at a rate of γ_1 (processes shown by a curved dotted arrow marked as γ_1 in Fig. 2). Consequently, it is expected[26] that the additional L_{IR} could initiate replenishing processes (schematically shown in Fig. 2 by a thick curved arrow marked as IR_1) which should increase $I_{\mathrm{PL}}^{\mathrm{QD}}$. As follows from our data, $R_{\mathrm{QD}}=1$ (i.e., $I_{\mathrm{PL}}^{\mathrm{QD}}$ remains unchanged) in the entire region $h\nu_{ex}\leqslant h\nu_{me}$, which corresponds to the case when carriers and excitons have been excited directly into the QD. These experimental findings allow us to exclude any possible influence of nonradiative processes on the carrier and excitons (i.e., affecting $I_{\mathrm{PL}}^{\mathrm{QD}}$ or R_{QD}) which have already been captured into the QD.

To have a nonvanishing value of the nonradiative recombination rate γ_1, at least one defect (DL) atom should be located in the very close [$\leqslant$10 nm (Ref. 19)] vicinity of a QD, which implies a rather high concentration ($\sim 10^{12}$ cm^{-2}) of such defects in the plane of the WL. In the rest of this section we will mainly analyze the regions of the $h\nu_{ex}$'s where $R_{\mathrm{QD}}<(>)1$. For the sake of simplicity, we will denote them as $h\nu_{ex}<h\nu_{th}$ ($h\nu_{ex}>h\nu_{th}$), having in mind that these really correspond to the excitation energy regions of $h\nu_{me}<h\nu_{ex}<h\nu_{th}^{\mathrm{Si}}$ ($h\nu_{th}^{\mathrm{C}}<h\nu_{ex}<E_{\mathrm{X}}^{\mathrm{GaAs}}$), respectively.

B. $h\nu_{ex}<h\nu_{th}$

We will continue the analysis considering the region of $h\nu_{ex}<h\nu_{th}$. To account for the L_{IR}-induced changes of $I_{\mathrm{PL}}^{\mathrm{WL}}$ [Fig. 3(b)] we consider defects, located in the WL, causing nonradiative recombination. They can capture excitons in the WL with a nonradiative capture rate γ_2, as schematically shown in Fig. 2. After that, the captured excitons can either recombine at a recombination rate γ_3 or be excited back into the WL by means of the absorption of the light of the L_{IR}, as shown in Fig. 2 by the thick solid arrow marked as IR$_2$. To analyze the evolution of $I_{\mathrm{PL}}^{\mathrm{QD}}$ and $I_{\mathrm{PL}}^{\mathrm{WL}}$, induced by the illumination of the additional IR laser, we consider the rate equations for the total number of excitons captured into the QD, n_{QD}, the total number of free excitons in the excited volume of the WL, n_{WL}, and the total number of defects, which have captured excitons excited in the WL, N_c:

$$\frac{dn_{\mathrm{WL}}}{dt} = +g_{\mathrm{WL}} + N_c w_2 - n_{\mathrm{WL}}\gamma_2 - \frac{n_{\mathrm{WL}}}{\tau_R} - n_{\mathrm{WL}}\gamma_c, \quad (1a)$$

$$\frac{dN_c}{dt} = +n_{\mathrm{WL}}\gamma_2 - N_c\gamma_3 - N_c w_2, \quad (1b)$$

$$\frac{dn_{\mathrm{QD}}}{dt} = +n_{\mathrm{WL}}\gamma_c - \frac{n_{\mathrm{QD}}}{\tau_r^{\mathrm{QD}}}, \quad (1c)$$

where $g_{\mathrm{WL}}=d_{\mathrm{WL}}\alpha_{\mathrm{WL}}P_0/h\nu_{ex}$ and $w_2=(\sigma^{ex}P_{\mathrm{IR}})/(h\nu_{\mathrm{IR}}S)$ are the generation rate for free excitons due to the band-to-band absorption initiated by the laser L_0 and the probability per defect and time unit to excite the captured exciton back to the WL (with the corresponding optical cross section σ^{ex}) as a result of the IR laser absorption, respectively. d_{WL} is the thickness of the WL in the growth direction, α_{WL} is the absorption coefficient of the InAs material, and S is the area of the laser spot. The last two terms in Eq. (1a) describe the processes of the radiative recombination of n_{WL} (with a recombination time τ_R) and the capture of n_{WL} into the QD with a capture probability γ_c, respectively. The first term in Eq. (1c) describes the generation processes of excitons into the QD and the last term describes the processes of the radiative recombination which are measured in the experiment as $I_{\mathrm{PL}}^{\mathrm{QD}}$. No terms which could account for the nonradiative recombination of the n_{QD} are introduced in Eq. (1) for reasons discussed above. The steady-state solution of Eq. (1c) results in

$$I_{\mathrm{PL}}^{\mathrm{QD}} = \frac{n_{\mathrm{QD}}}{\tau_r^{\mathrm{QD}}} = n_{\mathrm{WL}}\gamma_c = I_{\mathrm{PL}}^{\mathrm{WL}}\gamma_c\tau_R = g_{\mathrm{QD}}, \quad (2)$$

where g_{QD} can be regarded as a generation rate into the QD. The typical value of the ratio $I_{\mathrm{PL}}^{\mathrm{QD}}/I_{\mathrm{PL}}^{\mathrm{WL}}$ is considerably less than 1, as can be seen in Fig. 3(c) for the case of excitation with only L_0. This is even more valid when the L_{IR} is switched on: it increases $I_{\mathrm{PL}}^{\mathrm{WL}}$ and considerably decreases $I_{\mathrm{PL}}^{\mathrm{QD}}$ as is shown in Figs. 3(b) and 3(a), respectively. Thus, we consider $\tau_R^{-1} \gg \gamma_c$ and, consequently, can exclude the last term in Eq. (1a) from further analysis. Within this approximation, the steady-state solutions of Eqs. (1a) and (1b) result in

$$I_{\mathrm{PL}}^{\mathrm{WL}}(P_{\mathrm{IR}}) = \frac{n_{\mathrm{WL}}}{\tau_R} = g_{\mathrm{WL}}\frac{1+w_2/\gamma_3}{1+w_2/\gamma_3+\gamma_2\tau_R}, \quad (3a)$$

$$R_{\mathrm{WL}} = \frac{I_{\mathrm{PL}}^{\mathrm{WL}}(P_{\mathrm{IR}})}{I_{\mathrm{PL}}^{\mathrm{WL}}(P_{\mathrm{IR}}=0)} = \frac{(1+w_2/\gamma_3)(1+\gamma_2\tau_R)}{1+w_2/\gamma_3+\gamma_2\tau_R}. \quad (3b)$$

It is clear that $I_{\mathrm{PL}}^{\mathrm{WL}}$ and R_{WL} can only increase with w_2 (i.e., with P_{IR}) achieving an upper limit of g_{WL} and $1+\gamma_2\tau_R$, respectively. Such an enhancement of the PL signal induced by below band gap excitation was previously demonstrated[27] for the case of epitaxially grown bulk GaAs. Consequently, to explain the decrease of $I_{\mathrm{PL}}^{\mathrm{QD}}$, induced by the IR laser, we need, according to Eq. (2), to consider γ_c to be essentially reduced by the L_{IR}. Here we implicitly assume τ_R to be independent of the IR laser illumination. Then, combining Eqs. (2), (3a), and (3b), we can express R_{QD} in the following form:

$$R_{\mathrm{QD}} = \frac{I_{\mathrm{PL}}^{\mathrm{QD}}(P_{\mathrm{IR}})}{I_{\mathrm{PL}}^{\mathrm{QD}}(P_{\mathrm{IR}}=0)} = R_{\mathrm{WL}}\frac{w_c(P_{\mathrm{IR}})}{w_c(P_{\mathrm{IR}}=0)}, \quad (4)$$

where $w_c=\gamma_c\tau_R$ is the dimensionless parameter called collection efficiency of the particles from the WL into the QD. In what follows we present a model which could account for the considerable decrease of w_c, induced by the IR laser, with respect to the value of $w_c(P_{\mathrm{IR}}=0)$.

First, the dependence of the $w_c(P_{\mathrm{IR}}=0)$ on the $h\nu_{ex}$ [Fig. 3(c)] should be emphasized. It is seen that the collection efficiency acquires two averaged values of 0.03 and of $\approx$0.003 in the regions of $h\nu_{ex}<h\nu_{th}$ and $h\nu_{ex}>h\nu_{th}$, respectively. It would be reasonable to expect that the low value of w_c and, hence, the very weak value of $I_{\mathrm{PL}}^{\mathrm{QD}}$, registered in the last case, could be explained in terms of an enhanced role of the nonradiative recombination efficiency, which should result in a poor collection of carriers into the QD. However, if this were the case, then $I_{\mathrm{PL}}^{\mathrm{WL}}$ should also be reduced at $h\nu_{ex}>h\nu_{th}$ with respect to the value measured at $h\nu_{ex}<h\nu_{th}$. Evidently, this conclusion contradicts the PLE spectrum of the WL shown in Fig. 3(a). We also performed measurements detecting $I_{\mathrm{PL}}^{\mathrm{WL}}$ (integrated over the entire spectral region of the WL PL band) for a number of $h\nu_{ex}$'s (not shown here), which nicely reproduce the spectral features of the PLE spectrum in Fig. 3(a). In addition, if the nonradiative recombination were more efficient for $h\nu_{ex}>h\nu_{th}$, then, ac-

cording to Eq. (3b), R_{WL} should be higher with respect to the value acquired at $h\nu_{ex}<h\nu_{th}$. Indeed, in the high limit of P_{IR}, $R_{\mathrm{WL}}=1+\gamma_2\tau_R$, as explained above. Consequently, the higher value of the nonradiative rate γ_2, the greater value of R_{WL} is expected. The values of R_{WL} of 1.1 and 2.5, obtained for $h\nu_{ex}>h\nu_{th}$ and $h\nu_{ex}<h\nu_{th}$ [Fig. 3(b)], show, on the contrary, that the nonradiative recombination is more efficient at $h\nu_{ex}<h\nu_{th}$. Accordingly, the greater collection efficiency, observed in the experiment [Fig. 3(c)], should be accompanied by a higher value of γ_2 [Fig. 3(b)], which also contradicts the above given suggestion. Consequently, some other considerations have to be employed to explain the considerably lower values of $w_c(P_{\mathrm{IR}}=0)$ at $h\nu_{ex}>h\nu_{th}$ [Fig. 3(c)].

The remarkable difference between the cases of excitation with a single L_0 at $h\nu_{ex}>h\nu_{th}$ and at $h\nu_{ex}<h\nu_{th}$ is the simultaneous generation of surplus e's in the former case (the processes shown by arrow 3 in Fig. 2). It is important to note that the analogous situation is achieved when, in addition to the L_0, exciting at $h\nu_{ex}<h\nu_{th}$, the IR laser is switched on. Indeed, in addition to the equal amount of e's and h's, created by the L_0 in this case, some amount of surplus holes is created in the sample as a result of the absorption of the IR laser light. The only difference between these two cases is that in the former case an extra amount of e's has been created, while in the latter surplus h's have been formed. Consequently, both effects—the reduction of the $w_c(P_{\mathrm{IR}}=0)$ at $h\nu_{ex}>h\nu_{th}$ [Fig. 3(c)] and the decrease of $I_{\mathrm{PL}}^{\mathrm{QD}}$, initiated by the IR laser for the case with L_0 excitation at $h\nu_{ex}<h\nu_{th}$ [Fig. 3(a)]—should be explained in terms of the effect of extra free charge generation.

We propose the following model to explain the influence of the extra charge on the collection efficiency of the photocreated carriers from the WL into the QD. We assume the existence of an electric field F with direction in the plane of the WL. Photoexcited e's and h's move along the plane of the WL for some time, decreasing their kinetic energy until they bind together and recombine as excitons, contributing to $I_{\mathrm{PL}}^{\mathrm{WL}}$. The QD can thus be populated with carriers and excitons only for the case when the capture time from the WL into the QD is less than the time mentioned above. The efficiency of the $e(h)$ transport can be quantitatively characterized by a mean free path $l_{e(h)}$, which can be expressed by $l_{e(h)}=V_{e(h)}\tau_{e(h)}$, where $\tau_{e(h)}$ is the average time between the two consecutive scattering events and $V_{e(h)}$ is the velocity of the $e(h)$. The existence of a built-in electric field F, in the plane of the WL, results in a drift velocity $V_{e(h)}^{dr}=\mu_{e(h)}F$ of carriers, where $\mu_{e(h)}$ corresponds to the $e(h)$ mobility. If the excited carriers are subjected to this field, they are expected to acquire rather high $V_{e(h)}=V_{e(h)}^{dr}$, which results in an efficient carrier transport along the plane of the WL and, consequently, a rather high collection efficiency is expected in this case. According to our model, the generation of an extra amount of free charge (e's or h's) effectively compensates F and, consequently, reduces $V_{e(h)}$ down to the thermal velocity $V_{e(h)}^{T}=(2k_BT/m_{e(h)})^{1/2}$, where k_B is the Boltzmann constant and $m_{e(h)}$ is the $e(h)$ effective mass. This leads to a considerably less efficient carrier transport along the WL plane, which results in a decrease of $I_{\mathrm{PL}}^{\mathrm{QD}}$.

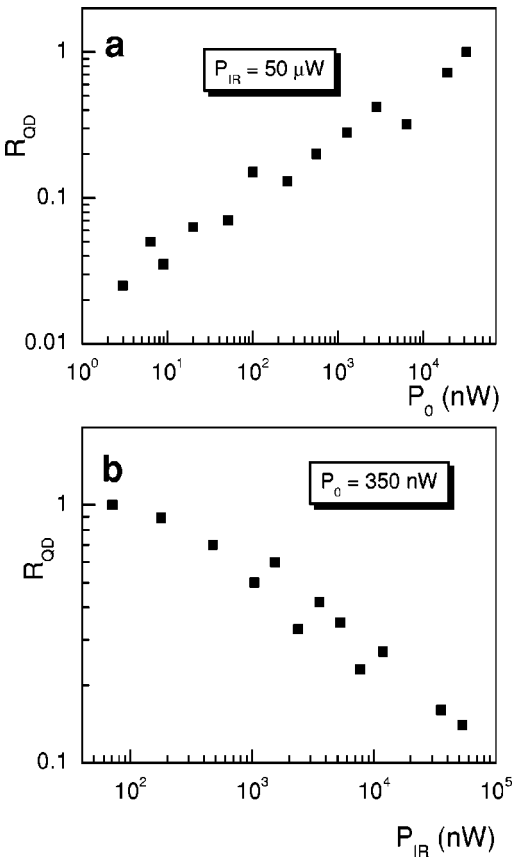

FIG. 4. (a) The ratio of the spectrally integrated PL intensities of the QD (R_{QD}) measured with both lasers and the integrated PL intensities measured with only laser L_0, at $T=5$ K, $h\nu_{ex}=1.470$ eV, $P_{\mathrm{IR}}=50$ μW as a function of P_0. (b) R_{QD} measured at $T=5$ K, $h\nu_{ex}=1.470$ eV, $P_0=350$ nW as a function of P_{IR}.

Accordingly, we explain the IR-laser-induced decrease of $I_{\mathrm{PL}}^{\mathrm{QD}}$ ($R_{\mathrm{QD}}<1$) registered at $h\nu_{ex}<h\nu_{th}$ [shown in Fig. 3(a)] and a reduced value of $w_c(P_{\mathrm{IR}}=0)$ obtained at $h\nu_{ex}>h\nu_{th}$ [Fig. 3(c)] in terms of an effective screening of the internal electric field F by the surplus h's and e's generated in the sample at the experimental conditions corresponding to the former and latter cases, respectively. When the surplus $h(e)$ appear in the WL, the carrier will move along (opposite to) the direction of the built-in field. If the carrier $h(e)$ is localized at the interface potential fluctuations, the $h(e)$ will stay there for a rather long time, providing an effective screening of the initial field F. Screening of the internal field can also be achieved when equal numbers of h's and e's are created in the sample, but a rather high carrier concentration is needed for this. The less effective screening in the last case could be understood by taking into account the radiative recombination processes, which prevent the localized carrier state to survive for a long time.

Figure 4 shows R_{QD} measured at $T=5$ K and $h\nu_{ex}=1.470$ eV as a function of both P_0 (a) and P_{IR} (b), respectively. It is seen that it progressively approaches 1 with decreasing P_{IR} [Fig. 4(b)]. This behavior is expected, since the decrease of the P_{IR} (reducing of the concentration of the surplus h's) should result in a less efficient screening of the

built-in field. Figure 4(a) shows a gradual increase of R_{QD} up to the value of 1 with the increase of the P_0 at a fixed maximum value of the $P_{\mathrm{IR}}=50\ \mu$W. This behavior is also consistent with our model. Indeed, if the carrier concentration, generated by the L_0, becomes rather high to completely screen the internal field, then the additional holes which appear after that the IR laser has been switched on cannot compensate it more.

To estimate the value of F needed to obtain the values of R_{QD} measured in the experiment, we use the following considerations. The dimensionless parameter w_c, which, according to Eq. (2), is the ratio between the integrated intensities $I_{\mathrm{PL}}^{\mathrm{QD}}$ and $I_{\mathrm{PL}}^{\mathrm{WL}}$, can be expressed in the form S_c/S, where $S_c=l_{e(h)}^2$ could be understood as the total area, from which the QD can collect carriers, excited in the plane of the WL. Such an expression for w_c is justified by the idea that all carriers which are excited in the plane of the WL within the area of the laser spot S contribute to $I_{\mathrm{PL}}^{\mathrm{WL}}$, while only a small fraction of them, which are able to be captured into the QD, will initiate $I_{\mathrm{PL}}^{\mathrm{QD}}$. Using these considerations, we rewrite Eq. (4) in the following form:

$$R_{\mathrm{QD}}=R_{\mathrm{WL}}\frac{S_c(P_{\mathrm{IR}}=P_{\mathrm{IR}}^{\max})}{S_c(P_{\mathrm{IR}}=0)}=\left(\frac{V_{e(h)}^T}{\mu_{e(h)}F}\right)^2 R_{\mathrm{WL}}. \qquad (5)$$

This equation allows one to directly estimate the value of the electric field F only if the values of the $e(h)$ mobility were known. To calculate the lowest limit of F we will consider the heaviest particle: i.e., the hole. We employ the value of the in-plane effective mass $m_{h\|}=0.155m_0$ (m_0 is the mass of the free electron), as was derived in the experiment[34] for the case of ultrathin InAs quantum wells (QW's) embedded between two GaAs barriers. Since the measured and calculated values of the μ_h for the structure under study—ultrathin (thickness of 0.5 nm) InAs QW's—are not available in the literature, we have instead succeeded to measure the diffusion constant of the excitons (D_{ex}), which propagate along the plane of the WL. As a rough estimate we set the h diffusion coefficient D_h to be equal to the D_{ex}. This is justified by the conclusion, that the excitonic transport along the plane of the QW is mainly determined by the transport of the heaviest particle in the exciton, as was demonstrated for the InGaAs/GaAs (Ref. 13) and GaAs/AlGaAs (Ref. 35) systems.

In the measurements of D_{ex} we registered $I_{\mathrm{PL}}^{\mathrm{QD}}$ in the geometry employed for an experiment, when the exciting laser spot was set at different distances y from the QD position, as schematically shown in the inset in Fig. 5. Only those excitons $n_{\mathrm{WL}}(y)$ which are able to reach the QD during the decay time τ_{d} ($\tau_{\mathrm{d}}^{-1}=\tau_R^{-1}+\gamma_2$), propagating over the distance y along the plane of the WL, will contribute to the measured $I_{\mathrm{PL}}^{\mathrm{QD}}$, which is related to the $n_{\mathrm{WL}}(y)$ by means of Eq. (2). Here we assume that the collection efficiency will not be changed when moving the laser spot aside of the QD at different distances. This can be justified by the following arguments. For the current measurements, $h\nu_{ex}>h\nu_{th}$ has been chosen, providing the simultaneous generation of extra e's in the volume of the GaAs barriers. These surplus e's were able

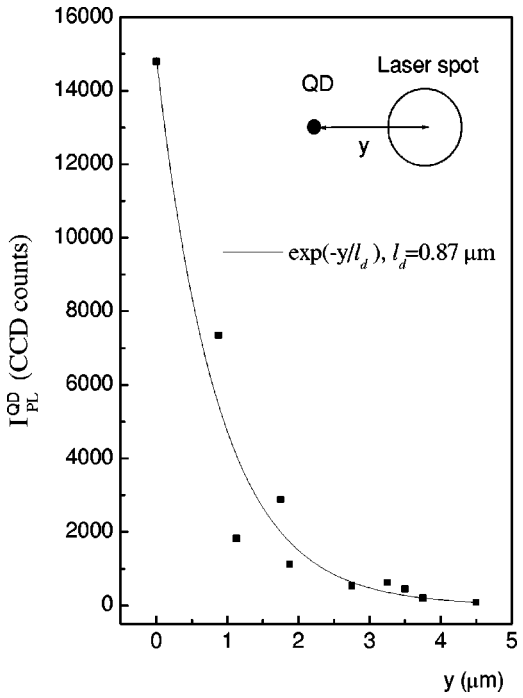

FIG. 5. The symbols show the spectrally integrated PL intensity of the QD, $I_{\mathrm{PL}}^{\mathrm{QD}}$, measured with only one laser L_0 at $T=5$ K, $h\nu_{ex}=1.5$ eV, and $P_0=500$ nW for a number of displacements y between the center of the laser spot and the position of the QD. The solid line corresponds to the exponential decay fitted to the data. The inset shows schematically the experimental arrangement.

to propagate over distances of several μm, as was experimentally demonstrated in our previous publication.[28] Consequently, the same conditions apply for the carrier-exciton collection into the QD, which concerns the presence of extra charges even at different positions of the spot of L_0 with respect to the QD location. To find the value of $n_{\mathrm{WL}}(y,t)$, we consider the continuity equation, which for this case is transformed into a one-dimensional diffusion equation supplemented by a linear decay term[35] for $n_{\mathrm{WL}}(y,t)$:

$$\frac{dn_{\mathrm{WL}}(y,t)}{dt}=D_{ex}\frac{d^2n_{\mathrm{WL}}(y,t)}{d^2y}-\frac{n_{\mathrm{WL}}(y,t)}{\tau_{\mathrm{d}}}. \qquad (6)$$

The steady-state solution of Eq. (6) could be obtained as $n_{\mathrm{WL}}(y)=n_{\mathrm{WL}}(y=0)\exp(-y/l_{\mathrm{d}})$, where $l_{\mathrm{d}}=(D_{ex}\tau_{\mathrm{d}})^{1/2}$ is the diffusion length of an exciton and $n_{\mathrm{WL}}(y=0)$ can be found from Eq. (3a). The data shown in Fig. 5, measured at $T=5$ K, $h\nu_{ex}=1.5$ eV, and $P_0=500$ nW, have been nicely fit by a simple exponential decay function with the fitting parameter $l_{\mathrm{d}}=0.87\ \mu$m. We have performed the same measurements for a number of $h\nu_{ex}$'s. The values of l_{d} obtained varied in the range between 0.82 and 1.34 μm. Consequently, the value of $l_{\mathrm{d}}=1\ \mu$m was chosen in the following estimate. A value of $\tau_{\mathrm{d}}=300$ ps has been measured for InGaAs/GaAs thin QW's for the case of $h\nu_{ex}<E_{\mathrm{X}}^{\mathrm{GaAs}}$ (Ref. 30). This decay time τ_{d} was employed as the input value to evaluate the diffusion constant D_{ex}. To calculate μ_h, we use the Einstein relation $\mu_h k_B T=eD_h$, where e is the elementary charge. Finally, inserting the values of $R_{\mathrm{QD}}=0.05$ and

$R_{WL}=2.5$ [Figs. 3(a) and 3(b), respectively] into Eq. (5), a value of $F=280$ V/cm was evaluated. In fact, Fig. 4(a) shows the minimum value of $R_{QD}=0.025$, achieved for $P_0=3$ nW. The corresponding value of R_{WL} (not shown here) also equals 2.5, which allows an estimate of the lowest field limit as being 400 V/cm. This value is well below the reported values for the electric field of 10^4 V/cm, which was revealed for analogously grown InGaAs/GaAs samples.[36]

The exact origin of this built-in field is not known at the moment and further studies are needed to reveal its nature. The origin is believed to be due to the defects (donors and acceptors) which are positioned at the InAs/GaAs interface around the QD. The existence of such defects was reported previously.[14] In full darkness an e from the donor atom can be captured by an acceptor interfacial defect, giving rise to the appearance of a built-in field F in the plane of the WL as a result of charge localization on space-separated defects. To calculate the distance r between two space-separated charges, which could give rise to a field of $F=400$ V/cm between them, we used Coulomb's law for the electric field distribution, produced by a point charge. A dielectric constant of 12.6 (Ref. 32) was used, which results in $r=140$ nm. This is 4 times longer than the base diameter (35 nm) of the QD and implies an areal defect concentration of 5×10^9 cm^{-2}, corresponding to a limited number (2–10) of defects per ''collection area'' of a QD. This concentration is well below the calculated value of the areal defect concentration (10^{12} cm^{-2}), which is needed to effectively capture carriers and excitons from the QD. Thus, we conclude that the idea of a defect-induced built-in electric field in the plane of the WL is consistent with our experimental observations that the IR laser does not influence I_{PL}^{QD} at $h\nu_{ex}<h\nu_{me}$. It should be mentioned that the relative decrease of I_{PL}^{QD} with respect to I_{PL}^{WL} initiated by a magnetic field directed perpendicular to the plane of the WL, observed in an experiment of a large ensemble of InAs/GaAs QD's,[15] was also explained in terms of a reduced lateral (in the plane of the WL) carrier transport, causing a decreasing capture of carriers from the WL into the QD's.

C. $h\nu_{ex}>h\nu_{th}$

Now we turn to the discussion of the increase of I_{PL}^{QD} ($R_{QD}>1$) detected at $h\nu_{ex}>h\nu_{th}$ [Fig. 3(a)]. Here the situation is opposite to what has already been discussed. Consequently, some other additional considerations have to be taken into account to explain the observed phenomenon. We recall, first, that at excitation energies $h\nu_{ex}>h\nu_{th}$, an extra amount of free e's is generated. These e's should, according to the suggested model, effectively screen the lateral field F. Consequently, when the second IR laser illuminates the sample, generating an extra amount of free h's, the collection efficiency into the QD is not expected to be further reduced, leading to a decrease of I_{PL}^{QD}. On the contrary, the appearance of extra holes in the sample is expected to initiate some increase of I_{PL}^{QD}, resulting in $R_{QD}>1$. This prediction stems from the fact that at the excitation conditions of $h\nu_{ex}>h\nu_{th}$, the QD has already been populated with extra e's, a fact which is proved by the observation of the totally ''negative'' PL spectra, consisting of lines of the negatively charged exciton [Fig. 1(e)]. Consequently, it is reasonable to expect that the negatively charged QD will effectively attract extra positive charges, giving rise to an increase of I_{PL}^{QD}. This idea is supported by the value of $R_{QD}>1$, derived for $h\nu_{ex}>h\nu_{th}$ [Fig. 3(a)].

In order to explain the increase of I_{PL}^{QD}, initiated by the IR laser, we introduce the generation factor g_{ad} in addition to g_{QD}, which could be achieved by exciting only with the laser L_0. Combining Eqs. (2) and (3a), it is easy to show that $g_{QD}=g_{WL}w_c$, if we neglect the term $\gamma_2\tau_R$ with respect to 1 in Eq. (3a), because it gives a contribution essentially less than one in the region of $h\nu_{ex}>h\nu_{th}$, as was explained above. To obtain a value of $R_{QD}\approx5$ [shown in Fig. 3(a)] we need to assume that $g_{ad}/g_{QD}\approx4$, because the measured R_{QD}, according to this model, should be expressed in the form

$$R_{QD}=\frac{g_{QD}+g_{ad}}{g_{QD}}. \tag{7}$$

Figure 6 shows the values of R_{QD}, measured at $T=5$ K, $h\nu_{ex}=1.503$ eV, and (a) at a fixed $P_{IR}=P_{IR}^{max}=50$ μW and various P_0's and (b) at a fixed $P_0=17$ nW and a number of P_{IR}'s, respectively. It is seen [Fig. 6(b)] that for a fixed P_0 the increase of the P_{IR} will leave R_{QD} unchanged up to $P_{IR}=10$ μW, followed by a linear increase of R_{QD} for higher values of the P_{IR}. R_{QD} exhibits a more complex behavior, as revealed in Fig. 6(a): Starting from the lowest P_0's, R_{QD} first increases to reach a maximum value of 5.2 for $P_0=P_0^*=17$ nW and then gradually decreases for higher values of P_0. The decrease of R_{QD}, shown in Fig. 6(a), can be understood from Eq. (7) in the following way: At $P_0=P_0^*$, g_{ad} has reached its maximum value and, correspondingly, does not increase further with increasing P_0, while g_{QD} still increases. To explain such a behavior of g_{ad} we would like to recall the fact that it was introduced as an exciton generation rate, i.e., generation rate of pairs (both e's and h's) into the QD. For the experimental conditions described, the surplus e's and h's are generated separately, as a result of the absorption of excitation light from two different lasers L_0 and L_{IR} and, correspondingly, with two different generation rates g_e and g_h, respectively. Both g_e and g_h are linearly proportional to the excitation power P_0 and P_{IR} of the corresponding laser. However, in order to contribute to the g_{ad}, creation of both e and h in the QD is needed. Consequently, g_{ad} is determined by the lowest value of g_e and g_h in the double-excitation experiments.

The generation rate g_e of extra electrons from the acceptor atoms located in the GaAs barriers and the generation rate g_{QD} can be expressed in the form $g_e=\sigma_e N_a d_{GaAs}P_0/h\nu_{ex}$ and $g_{QD}=w_c g_{WL}=w_c\alpha_{WL}d_{WL}P_0/h\nu_{ex}$. Here d_{GaAs} (d_{WL}) $=200$ nm (0.5 nm) is the thickness of the GaAs barriers (WL) in the growth direction, $\sigma_e=3.5\times10^{-15}$ cm^2 is the optical cross section, as was calculated (based on formulas given in Ref. 37) for the C acceptor, $T=5$ K and $h\nu_{ex}=1.503$ eV, N_a is the bulk acceptor concentration, and $\alpha_{WL}=10^4$ cm^{-1} (Ref. 38) is the absorption coefficient of

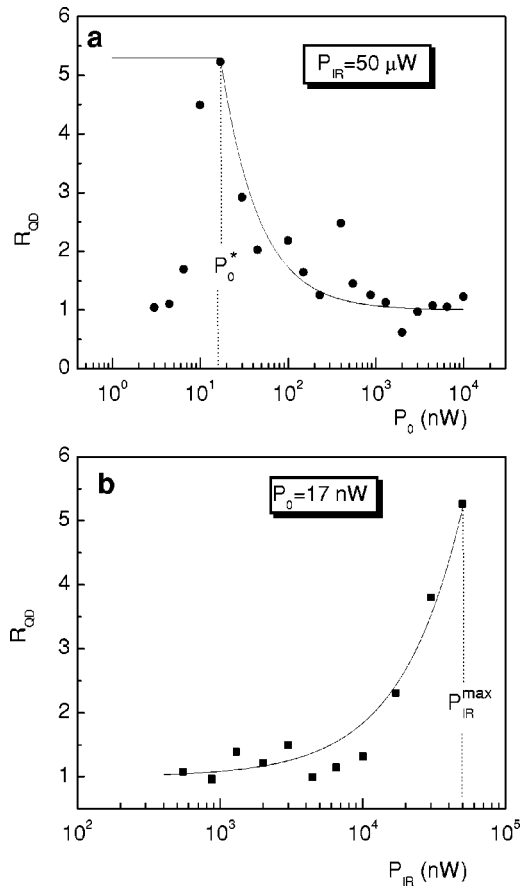

FIG. 6. (a) The symbols show the ratio (R_{QD}) of the spectrally integrated PL intensities of the QD measured with both lasers and the PL intensities measured with only one laser L_0 measured at $T=5$ K, $h\nu_{ex}=1.503$ eV, $P_{\mathrm{IR}}=50\ \mu$W for a number of P_0's. The solid line is the result of calculations based on Eqs. (8a) and (8b). (b) The symbols show the values of R_{QD} measured at $T=5$ K, $h\nu_{ex}=1.503$ eV, $P_0=17$ nW for a number of P_{IR}'s. The solid line is the result of calculations based on Eq. (9).

InAs. To obtain $R_{\mathrm{QD}}=5.2$, the maximum value of R_{QD} shown in Fig. 6(a), it is required that $g_{ad}/g_{\mathrm{QD}}=g_e/g_{\mathrm{QD}}=4.2$ [according to Eq. (7)]. This value can be achieved using the experimental value of $w_c=1.7\times10^{-3}$ [Fig. 3(c)] and assuming that $N_a=5\times10^{13}$ cm^{-3}. The latter concentration agrees well with the value of the Si acceptor concentration in the GaAs barriers of 10^{13} cm^{-3}, which was used as an adjustable parameter to fit the experimental data in our previous work.[28] The concentration of C acceptors should considerably exceed the Si concentration in MBE-grown GaAs.[39]

The generation rate for holes can be expressed in a similar way: $g_h=\sigma_h N_{\mathrm{DL}} d_{\mathrm{GaAs}} P_{\mathrm{IR}}/h\nu_{\mathrm{IR}}$, where σ_h is the optical cross section for the creation of free hole (processes shown by arrow IR_3 in Fig. 2) and N_{DL} is the concentration of the deep levels in the GaAs barriers. In spite of the fact that the typical value of N_{DL} is less than 10^{13} cm^{-3} in MBE-grown GaAs (Ref. 40) and that $\sigma_h\approx10^{-17}$ cm^2 (Ref. 25), is 2–3 orders of magnitude less than the above calculated σ_e, comparable values of g_e and g_h could be achieved for our experimental conditions ($P_0=17$ nW and the essentially higher $P_{\mathrm{IR}}^{\max}=50\ \mu$W).

Based on a statement given above, it is obvious that g_e should develop linearly with P_0. Accordingly, the only reason for the saturation of g_{ad} at $P_0=P_0^*$ is that $g_e(P_0=P_0^*)=g_h(P_{\mathrm{IR}}^{\max})$. In other words, for $P_0=P_0^*$, the total number of surplus e's becomes equal to that of extra holes. Consequently, for a further increase of P_0, g_{ad} cannot increase more and, hence, according to Eq. (7), only a decrease of R_{QD} is expected. To summarize the above ideas, the evolution of R_{QD} with P_0 could be expressed in the following form:

$$R_{\mathrm{QD}}=\frac{g_{\mathrm{QD}}+g_e}{g_{\mathrm{QD}}}=5.2,\quad P_0\leqslant P_0^*, \tag{8a}$$

$$R_{\mathrm{QD}}=1+4.2\frac{P_0^*}{P_0},\quad P_0>P_0^*. \tag{8b}$$

The values of R_{QD}, as evaluated from Eqs. (8a) and (8b), are shown in Fig. 6(a) by a solid line. It is seen that the calculated curve nicely fits the R_{QD} data measured at $P_0>P_0^*$, which supports the proposed origin for the increase of R_{QD} as being due to the additional separate generation of e's by L_0 and h's by L_{IR}.

However, there is an evident discrepancy between the fitted curve and the experimental data for $P_0<P_0^*$ [Fig. 6(a)]. Instead of a constant value of $R_{\mathrm{QD}}=5.2$ [as expected from Eq. (8a)], R_{QD} is found to decrease with decreasing P_0. To explain this behavior, we remind that the IR laser is also expected to effectively screen the internal field, giving rise to a decrease of $I_{\mathrm{PL}}^{\mathrm{QD}}$, as discussed above in detail. For the lowest values of P_0, the total number of surplus e's is not expected to be sufficient to totally screen F. Consequently, for the lowest-P_0 regime, a twofold effect from the IR laser is expected: first, to further screen F (which gives rise to a decrease of R_{QD}) and, second, to increase $I_{\mathrm{PL}}^{\mathrm{QD}}$. Thus we explain the discussed deviation of the experimental data from the suggested model by these competing processes, initiated by the IR laser in the region of $P_0<P_0^*$ [Fig. 6(a)].

It is interesting to note that the considerable increase of R_{QD}, which is explained in terms of extra carrier generation, is not accompanied by an analogous increase of R_{WL}, but only by 5%–10% [Fig. 3(b)]. This difference can be understood as due to the mechanism with separate generation of e's and h's. Indeed, for usual experimental conditions—i.e., when the carriers are generated by the same laser—each e-h pair is created instantly as a result of the absorption of the same photon. This e-h pair will recombine rather shortly [on a typical time scale of 300 ps (Ref. 30)], annihilating as an exciton. In the case of separate generation of e's and h's with certain generation rates g_e and g_h, there is a considerable time, of the order of $g_e^{-1}(g_h^{-1})$, between the event of the e generation by the photon coming from the first laser and the event when the h is created as a result of the absorption of the photon from the second laser. Thus, for example, at $P_0=17$ nW $g_e=3\times10^5$ s^{-1} and, hence, $g_e^{-1}=3.3\ \mu$s. During such a long period of time the photocreated particle

is expected to relax to the lowest energy level in the excited crystal structure—i.e., in the QD in our case. Consequently, it will be positioned there until a charge of opposite sign is captured into the QD. These processes will give rise to the increase of $I_{\mathrm{PL}}^{\mathrm{QD}}$, while $I_{\mathrm{PL}}^{\mathrm{WL}}$ is left almost unchanged.

Now we turn to the discussion of the evolution of R_{QD} shown in Fig. 6(b). These data are taken at a fixed $P_0 = P_0^*$, and consequently g_e is fixed in this case. Due to this, g_{ad} is expected to be entirely determined by the value of g_h, which, in turn, linearly depends on P_{IR}. Taking Eq. (7) into account, together with the considerations used to derive Eqs. (8a) and (8b), we predict the following expression for R_{QD}:

$$R_{\mathrm{QD}} = 1 + \frac{4.2}{P_{\mathrm{IR}}^{\max}} P_{\mathrm{IR}}. \tag{9}$$

The curve, calculated on the basis of Eq. (9), is shown in Fig. 6(b) by a solid line. Evidently, it fits nicely with the experimental data, which supports the proposed model.

We would like to compare these data with those measured at $h\nu_{ex} < h\nu_{th}$ shown in Fig. 4(b). While R_{QD} remains almost unchanged for $h\nu_{ex} > h\nu_{th}$ up to $P_{\mathrm{IR}} = 10\ \mu$W [Fig. 6(b)], it is considerably (≈ 2 times) reduced already at $P_{\mathrm{IR}} = 1\ \mu$W with respect to the lowest values of the P_{IR}'s engaged [Fig. 4(b)]. In other words, remarkable changes are detected in the latter case despite the fact of a 10 times smaller value of g_h. This confusing circumstance can be explained by the following arguments. At $h\nu_{ex} < h\nu_{th}$ only surplus holes are created and, consequently, there is a deficit of e's for recombination. As a result, a larger concentration of h's is expected in the plane of the WL compared to the case of excitation at $h\nu_{ex} > h\nu_{th}$. This excess hole population produces an effective screening of the built-in field at a lower value of g_h with respect to those needed to give rise to the increase of $I_{\mathrm{PL}}^{\mathrm{QD}}$ at $h\nu_{ex} > h\nu_{th}$.

Furthermore, we present results which, in our opinion, serve as direct experimental proof of the existence of an additional separate carrier generation provided by the two lasers. Figure 7(a) shows two PL spectra of the QD, for which one was measured with excitation with a single L_0 at $P_0 = 20$ nW and $h\nu_{ex} = 1.508$ eV (solid line), while the second PL spectrum (dotted line) was measured together with an additional IR laser with $P_{\mathrm{IR}} = 50\ \mu$W. Figure 7(a) clearly illustrates that the addition of L_{IR} results in a redistribution of the PL spectrum in favor of the neutral exciton X line, as well as in a general increase of $I_{\mathrm{PL}}^{\mathrm{QD}}$. Then the spot of L_0 was moved aside of the QD by a distance of 2.5 μm. This distance was chosen in such a way that no contribution to the PL spectrum could be registered when exciting only with L_0 [solid line in Fig. 7(b)]. Excitingly, when the IR laser was switched on, in addition to L_0, a well-defined PL spectrum appeared, consisting of the neutral exciton X line [dotted line in Fig. 7(b)]. This phenomenon can only be explained under the assumption that the two lasers generate or supply the QD with charges of opposite sign: surplus e's from L_0 and surplus h's from L_{IR}.

Accordingly, we make the following conclusion: The observed phenomenon of $R_{\mathrm{QD}} > 1$ [Fig. 3(a)] and the effect of

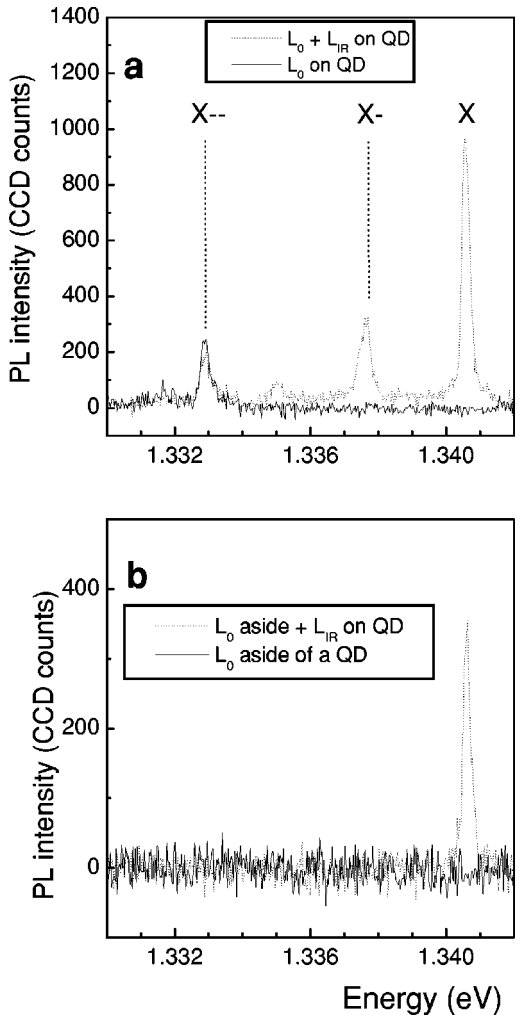

FIG. 7. PL spectra of a single QD measured at $T = 5$ K, $h\nu_{ex} = 1.508$ eV, $P_0 = 20$ nW, and $P_{\mathrm{IR}} = 50\ \mu$W for different excitation geometries: (a) The spots of the two lasers are both positioned on the QD. (b) The spot of L_{IR} is positioned on the QD, while the spot of the laser L_0 has been displaced 2.5 μm aside of the QD. The solid (dotted) line in (a) and (b) illustrates the PL spectrum measured with a single laser L_0 (both lasers).

the redistribution of the PL spectra in favor of the line X, initiated by the IR laser [Figs. 1(d) and 1(e)], should be explained in terms of a generation of surplus holes into the QD, rather than by the compensation effect of the surplus electrons somewhere in the crystal (i.e., outside of the QD).

Eventually we can summarize the proposed model as follows. The observed decrease of $I_{\mathrm{PL}}^{\mathrm{QD}}$ ($R_{\mathrm{QD}} < 1$) measured at $h\nu_{ex} < h\nu_{th}$ [Fig. 3(a)] is explained in terms of an effective screening of the lateral internal field by surplus h's, while the considerable increase of $I_{\mathrm{PL}}^{\mathrm{QD}}$ ($R_{\mathrm{QD}} > 1$) for $h\nu_{ex} > h\nu_{th}$ [also shown in Fig. 3(a)] is due to an additional generation of carriers into the QD. Note that excitation with solely L_{IR} does not give any detectable PL signal.

Obviously, this model predicts no changes caused by the IR laser in the excitation energy region of $h\nu_{ex} \leqslant h\nu_{me}$, because carriers and excitons are excited directly into the QD at these experimental conditions and, hence, are not subjected

to the transport along the plane of the WL, prior to the capture into the QD. The only effect of the IR laser in this case is to supply the QD with extra holes. Consequently, the interpretation of the line X^* shown in Figs. 1(b) and 1(c) in terms of the positively charged exciton seems reasonable.

The gradual increase of R_{QD} from 0.1 up to 1, as $h\nu_{ex}$ is progressively reduced in the region around the $E_{\mathrm{HH}}^{\mathrm{WL}}$ [Fig. 3(a)], can be explained by the monotonous decrease of the kinetic energy of the excited carriers, which approach zero at $h\nu_{ex}=h\nu_{me}$. The reduced kinetic energy assumes a faster carrier localization at the potential fluctuations of the InAs/GaAs interface, making their transport properties unaffected by the internal electric field and, consequently, they cannot be modified by the IR laser illumination.

Further we discuss the intermediate region of $h\nu_{ex}$'s around $h\nu_{ex}=1.485$ eV where $R_{\mathrm{QD}}=1$ [Fig. 3(a)]. In this region, the IR laser only redistributes the PL spectrum of the QD, making it more ''neutral,'' but does not initiate an increase of $I_{\mathrm{PL}}^{\mathrm{QD}}$. A typical example is shown in Fig. 1(d) for the case of $h\nu_{ex}=1.484$ eV. As seen in Fig. 3(a), this excitation energy is higher than the $h\nu_{th}^{\mathrm{Si}}$, but lower than that for the C acceptors. For these excitation conditions, $\sigma_e=6.7\times10^{-16}$ cm^2 (Ref. 37) results in a ratio of $g_e/g_{\mathrm{QD}}=0.16$, assuming, as explained above, a value of 10^{13} cm^{-3} for the concentration of the Si acceptor atoms. Consequently, g_{ad} is essentially less than g_{QD} in this case and, according to Eq. (7), no considerable increase of $I_{\mathrm{PL}}^{\mathrm{QD}}$ is expected.

We next discuss shortly the changes, induced by the IR laser, in the PL spectra of the QD obtained for a number of $h\nu_{ex}>E_{\mathrm{X}}^{\mathrm{GaAs}}$ in the range between 1.52 and 1.68 eV (not shown here). These changes were found to be identical for any of the $h\nu_{ex}$ in this range and entirely determined by the powers of the two lasers. In particular, for a fixed maximum value of P_{IR} and the lowest values of P_0, $I_{\mathrm{PL}}^{\mathrm{QD}}$ has been considerably quenched, while the quenching was progressively reduced with increasing P_0. These observations are satisfactorily explained by the suggested model of the internal electric field, analogously to the case of $h\nu_{ex}<h\nu_{th}$ [Fig. 4(a)], where an equal number of e's and h's was created in the sample. We note here that at the excitation with $h\nu_{ex}>E_{\mathrm{X}}^{\mathrm{GaAs}}$ we can consider equal amount of e's and h's to be created in the sample. This follows from the fact that one can neglect the concentration of the residual acceptor atoms with respect to the free density of states in GaAs. The most remarkable fact is that we were not able to register any increase of $I_{\mathrm{PL}}^{\mathrm{QD}}$ induced by the IR laser. This result can easily be understood if one evaluates the ratio of g_{ad}/g_{QD}, which could be expected for the case of $h\nu_{ex}>E_{\mathrm{X}}^{\mathrm{GaAs}}$. The only difference from the value of 4.2, obtained previously for the excitation in the WL, is that instead of $d_{\mathrm{WL}}=0.5$ nm in the denominator of the expression derived above we have to substitute $d_{\mathrm{GaAs}}=200$ nm, which results in $g_{ad}/g_{\mathrm{QD}}=0.01$.

We finally note that we assumed that most of the DL atoms, which absorb the IR laser light producing extra holes, are located in the GaAs barriers. This is justified by the considerably larger GaAs volume with respect to that of the WL, although the same processes shown by arrow IR_3 in Fig. 2 could take place in the volume of the WL as well. This fact will not qualitatively affect the proposed model.

IV. CONCLUSION

We have succeeded in revealing the role of the internal electric-field-driven mechanism of the carrier capture from the plane of the WL into the QD. This capture process is complementary to the mechanisms discussed up to date. The field is of great importance for experimental conditions when carriers are excited into the WL and, hence, must undergo a lateral transport prior to capture into the QD. The considerable changes in the PL spectra of the QD concerning the total intensity $I_{\mathrm{PL}}^{\mathrm{QD}}$ and also the distribution between different emission lines, induced by illumination of the sample with an additional IR laser, are suggested to be an effective tool to fabricate, e.g., QD-based optical switches.

ACKNOWLEDGMENTS

E.S.M. gratefully acknowledges financial support from the Wenner-Gren Foundations and partial support from the Russian Academy of Sciences (Low-Dimensional Nanostructures' 2003). V.D. is thankful to the Swedish Foundation for International Cooperation in Research and Higher Education (STINT) for financial support.

[1] D. Gammon, Nature (London) **405**, 899 (2000).

[2] L. Harris, D. J. Mawbray, M. S. Skolnick, M. Hopkinson, and G. Hill, Appl. Phys. Lett. **73**, 969 (1998).

[3] S. Maimon, E. Finkman, G. Bahir, S. E. Schacham, J. M. Garsia, and P. M. Petroff, Appl. Phys. Lett. **73**, 2003 (1998).

[4] T. Lundstrom, W. Schoenfeld, H. Lee, and P. M. Petroff, Science **286**, 2312 (1999); J. J. Finley, M. Skalitz, M. Arzberger, A. Zrenner, G. Bohm, and G. Abstreiter, Appl. Phys. Lett. **73**, 2618 (1998).

[5] D. Bimberg, M. Grundmann, and N. N. Ledentsov, *Quantum Dot Heterostructures* (Wiley, London, 1999).

[6] K. H. Schmidt, G. Medeiros-Ribeiro, J. M. Garcia, and P. M. Petroff, Appl. Phys. Lett. **70**, 1727 (1997); J. M. Garcia, T. Mankad, P. O. Holtz, P. J. Wellman, and P. M. Petroff, *ibid.* **72**, 3172 (1998); J. M. Garcia, G. Medeiros-Ribeiro, K. Schmidt, T. Ngo, J. L. Feng, A. Lorke, J. Kotthaus, and P. M. Petroff, *ibid.* **71**, 2014 (1997).

[7] R. Heitz, M. Veit, N. N. Ledentsov, A. Hoffmann, D. Bimberg, V. M. Ustinov, P. S. Kop'ev, and Zh. I. Alferov, Phys. Rev. B **56**, 10 435 (1997).

[8] A. W. E. Minnaert, A. Yu. Silov, W. van der Vleuten, J. E. M. Haverkort, and J. H. Wolter, Phys. Rev. B **63**, 075303 (2001); F. Findeis, A. Zrenner, G. Böhm, and G. Abstreiter, *ibid.* **61**, R10 579 (2000); R. Heitz, I. Mukhametzhanov, O. Stier, A. Madhukar, and D. Bimberg, Phys. Rev. Lett. **83**, 4654 (1999).

[9] B. Ohnesorge, M. Albrecht, J. Oshinowo, A. Forchel, and Y. Ar-

akawa, Phys. Rev. B **54**, 11 532 (1996); U. Bockelmann and T. Egeler, *ibid.* **46**, 15 574 (1992); A. Rack, R. Wetzler, A. Wacker, and E. Schöll, *ibid.* **66**, 165429 (2002); S. Raymond, K. Hinzer, S. Fafard, and J. L. Merz, *ibid.* **61**, 16 331 (2000); A. L. Efros, V. A. Kharchenko, and M. Rosen, Solid State Commun. **93**, 281 (1995).

[10] P. P. Paskov, P. O. Holtz, B. Monemar, J. M. Garcia, W. V. Schoenfeld, and P. M. Petroff, Jpn. J. Appl. Phys., Part 1 **40**, 2080 (2001).

[11] Y. Toda, O. Moriwaki, M. Nishioka, and Y. Arakawa, Phys. Rev. Lett. **82**, 4114 (1999).

[12] A. F. G. Monte, J. J. Finley, A. D. Ashmore, A. M. Fox, D. J. Mowbray, M. S. Skolnik, and M. Hopkinson, J. Appl. Phys. **93**, 3524 (2003).

[13] C. Lobo, R. Leon, S. Marcinkevičius, W. Yang, P. C. Sercel, X. Z. Liao, J. Zou, and D. J. H. Cockayne, Phys. Rev. B **60**, 16 647 (1999).

[14] S. Marcinkevičius, J. Siegert, R. Leon, B. Čechavičius, B. Magness, W. Taylor, and C. Lobo, Phys. Rev. B **66**, 235314 (2002); M. M. Sobolev, A. R. Kovsh, V. M. Ustinov, A. Yu. Egorov, A. E. Zhukov, M. V. Maksimov, and N. N. Ledentsov, Semiconductors **31**, 1074 (1997).

[15] S. Ménard, J. Beerens, D. Morris, V. Aimez, J. Beauvais, and S. Fafard, J. Vac. Sci. Technol. B **20**, 1501 (2002).

[16] S. Marcinkevičius, A. Gaarder, and R. Leon, Phys. Rev. B **64**, 115307 (2001).

[17] S. Marcinkevičius and R. Leon, Appl. Phys. Lett. **76**, 2406 (2000).

[18] P. W. Fry, J. J. Finley, L. R. Wilson, A. Lemaître, D. J. Mowbray, M. S. Skolnick, M. Hopkinson, G. Hill, and J. C. Clark, Appl. Phys. Lett. **77**, 4344 (2000).

[19] P. C. Sercel, Phys. Rev. B **51**, 14 532 (1995); X. Q. Li and Y. Arakawa, *ibid.* **56**, 10 423 (1997).

[20] A. Hartmann, Y. Ducommun, E. Kapon, U. Hohenester, and E. Molinari, Phys. Rev. Lett. **84**, 5648 (2000).

[21] P. Castrillo, D. Hessman, M. E. Pistol, J. A. Prieto, C. Pryor, and L. Samuelson, Jpn. J. Appl. Phys., Part 1 **36**, 4188 (1997); D. Bertram, M. C. Hanna, and A. J. Nozik, Appl. Phys. Lett. **74**, 2666 (1999).

[22] H. D. Robinson and B. B. Goldberg, Phys. Rev. B **61**, R5086 (2000).

[23] Q. X. Zhao, M. Willander, S. M. Wang, Y. Q. Wei, M. Sadeghi, and J. H. Yang, J. Appl. Phys. **93**, 1533 (2003).

[24] E. S. Moskalenko, K. F. Karlsson, P. O. Holtz, B. Monemar, W. V. Schoenfeld, J. M. Garcia, and P. M. Petroff, Phys. Rev. B **64**, 085302 (2001).

[25] P. Silverberg, P. Omling, and L. Samuelson, Appl. Phys. Lett. **52**, 1689 (1988).

[26] D. A. Mazurenko, A. V. Scherbakov, A. V. Akimov, A. J. Kent, and M. Henini, Semicond. Sci. Technol. **14**, 1132 (1999).

[27] A. V. Akimov and V. G. Shofman, J. Lumin. **53**, 335 (1992).

[28] E. S. Moskalenko, K. F. Karlsson, P. O. Holtz, B. Monemar, W. V. Schoenfeld, J. M. Garcia, and P. M. Petroff, Phys. Rev. B **66**, 195332 (2002).

[29] I. V. Ignatiev, I. E. Kozin, H. W. Ren, S. Sugou, and Y. Masumoto, Phys. Rev. B **60**, R14 001 (1999).

[30] G. Bacher, C. Hartmann, H. Schweizer, and H. Nickel, Solid State Commun. **95**, 15 (1995).

[31] Ph. Lelong and G. Bastard, Solid State Commun. **98**, 819 (1996); A. Wojs and P. Hawrylak, Phys. Rev. B **55**, 13 066 (1997).

[32] R. J. Warburton, B. T. Miller, C. S. Durr, C. Bodefeld, K. Karrai, J. P. Kotthaus, G. Medeiros-Ribeiro, P. M. Petroff, and S. Huant, Phys. Rev. B **58**, 16 221 (1998).

[33] M. Lomascolo, A. Vergine, T. K. Johal, R. Rinaldi, A. Passaseo, R. Cingolani, S. Patanè, M. Labardi, M. Allegrini, F. Troiani, and E. Molinari, Phys. Rev. B **66**, 041302 (2002); F. Findeis, M. Baier, A. Zrenner, M. Bichler, G. Abstreiter, U. Hohenester, and E. Molinari, *ibid.* **63**, 121309 (2001); R. J. Warburton, C. Schaflein, F. Haft, F. Bickel, A. Lorke, K. Karrai, J. M. Garcia, W. Schoenfeld, and P. M. Petroff, Nature (London) **405**, 926 (2000).

[34] J. Brübach, A. Yu. Silov, J. E. M. Haverkort, W. v. d. Vleuten, and J. H. Wolter, Phys. Rev. B **59**, 10 315 (1999).

[35] H. Hillmer, A. Forchel, S. Hansmann, M. Morohashi, E. Lopez, H. P. Meier, and K. Ploog, Phys. Rev. B **39**, 10 901 (1989).

[36] K. H. Schmidt, G. Medeiros-Ribeiro, M. Oestreich, P. M. Petroff, and G. H. Dohler, Phys. Rev. B **54**, 11 346 (1996); K. H. Schmidt, G. Medeiros-Ribeiro, and P. M. Petroff, *ibid.* **58**, 3597 (1998).

[37] W. P. Dumke, Phys. Rev. **132**, 1998 (1963).

[38] S. Adachi, J. Appl. Phys. **66**, 6030 (1989).

[39] I. H. Goodridge, *Properties of Gallium Arsenide* (Inspec, London, 1986).

[40] E. F. Schubert, *Doping in III-V Semiconductors* (Cambridge University Press, Cambridge, England, 1993).